Comput Geosci (2009) 13:349–361
DOI 10.1007/s10596-008-9123-9

ORIGINAL PAPER

Hybrid analytical and finite element numerical modeling of mass and heat transport in fractured rocks with matrix diffusion

Christopher I. McDermott · Robert Walsh · Ralph Mettier · Georg Kosakowski · Olaf Kolditz

Received: 23 September 2008 / Accepted: 25 November 2008 / Published online: 17 December 2008

Abstract Quantification of mass and heat transport in fractured porous rocks is important to areas such as contaminant transport, storage and release in fractured rock aquifers, the migration and sorption of radioactive nuclides from waste depositories, and the characterization of engineered heat exchangers in the context of enhanced geothermal systems. The large difference between flow and transport characteristics in fractures and in the surrounding matrix rock means models of such systems are forced to make a number of simplifications. Analytical approaches assume a homogeneous system, numerical approaches address the scale at which a process is operating, but may lose individual important processes due to averaging considerations. Numerical stability criteria limit the contrasts possible in defining material properties. Here, a hybrid analytical–numerical method for transport modeling in fractured media is presented. This method combines a numerical model for flow and transport in a heterogeneous fracture and an analytical solution for matrix diffusion. By linking the two types of model, the advantages of both methods can be combined. The methodology as well as the mathematical background are developed, verified for simple geometries, and applied to fractures representing experimental field conditions in the Grimsel rock laboratory.

Keywords Fractured rock · Matrix diffusion · Contaminant transport · Heat transport · Numerical modeling

C. I. McDermott (✉)
Edinburgh Collaborative of Subsurface Science and Engineering (ECOSSE), School of Geoscience, University of Edinburgh, West Mains Road, Edinburgh, EH9 3JW, Scotland
e-mail: cmcdermo@staffmail.ed.ac.uk

R. Walsh
INTERA Engineering, Ltd., 1 Raymond Street, Ottawa, ON, K1R 1A2 Canada

R. Mettier
Institute of Geology, University of Bern, Berne, Switzerland

G. Kosakowski
Paul Scherrer Institut, Villigen PSI, Villigen, Switzerland

O. Kolditz
Helmholtz Center for Environmental Research, Leipzig, Germany

1 Introduction

The profound understanding of flow and transport processes in fractured rock is often essential to the performance assessment of subsurface facilities, and robust models describing the transport of solutes and thermal energy in highly heterogeneous conductivity fields are of great interest, e.g., in geotechnical and geothermal engineering. In fractured rock, this problem is complicated by the combination of typically advective dominated transport in the rock fractures with diffusive dominated transport in the rock matrix surrounding the fractures.

Several key processes have been investigated numerically and experimentally regarding their impact on flow and transport properties in fractured media [1]. In a fractured rock mass, the distribution of fractures with

variable average permeability and orientation has a significant impact on the often anisotropic permeability and transport properties of a rock mass [2, 3]. Within the fractures themselves, channeling due to preferential flow pathways has a large influence on both flow and transport processes [4–6]. Permeability and velocity contrasts at the scale of both a rock mass and within an individual fracture can lead to the frequently observed tailing in solute breakthrough curves [7]. Often, the rock matrix surrounding a fracture has a much lower permeability than the fracture itself, but may strongly influence transport by acting as a reservoir into which solutes can diffuse and sorb. Diffusion and sorption in the matrix also cause tailing effects, and it can be difficult to distinguish the effects of variable velocity fields from those of matrix diffusion and sorption, particularly if both processes are operating in the same system at the same time [8].

Frequently, modelers use different processes to explain the observed tailing phenomena [9], and it can be quite difficult to devise a model that can adequately simulate both small-scale but large-magnitude permeability contrast within a fracture while also representing the diffusion and sorption of dissolved substances into the adjacent rock in a computationally efficient manner. By attempting to explain concentration breakthrough curves by invoking only matrix diffusion combined with advection and dispersion in an effective medium, there is a substantial risk of falsely characterizing the nature of transport processes in a given system, leading to incorrect predictions of the future behavior [10].

Researchers have developed analytical solutions for transport in fractured media based on the concept of matrix diffusion. Grisak and Pickens [11] presented an analytical model for advective solute transport in a planar fracture coupled with diffusive transport in the adjacent rock. Tang et al. [12] also demonstrated a solution for flow and transport in a planar fracture, but went further than Grisak and Pickens [11] by accounting for diffusion in the fracture, sorption processes, and radioactive decay. Subsequently, Sudicky and Frind [13] and Barker [14] developed solutions for matrix diffusion in an array of parallel planar fractures. These solutions have been applied for both fitting of field data and code verification during the development of numerical models, but they all share a common constraint. In order to obtain a purely analytical solution, it is necessary to neglect the effects of non-uniform aperture distributions within the fracture. This is problematic as it ignores the possibility that tailing effects are caused by heterogeneity as well as the evidence that spatial characteristics of the flow field influence matrix diffusion [15].

To achieve greater flexibility in the representation of physical processes that can be investigated in regarding their effect on transport in fractured systems, many investigators have turned to numerical models [9]. Several approaches for simulating heat and mass transport in fractured rock have been developed. Current trends are discussed in Neuman [16] and Berkowitz [7]. Although numerical techniques allow for the representation of irregular fracture geometry, which is not possible using a purely analytical technique, numerical simulations are truncated and can fail due to accuracy and stability problems. This is especially true where large differences in material parameters resulting in different dominant processes are present in the model and the equation solver can fail to converge. In fractured rock, the movement of solutes is characterized by advective dominated transport in the fractures and diffusive dominated transport in the matrix. Time-dependent solutions of advective and diffusive processes are controlled by different stability criteria. The optimal time-step lengths and elemental sizes to satisfy the Courant and Neumann stability criteria in advective dominated regions and diffusive dominated regions are quite different [17].

When discretely modeling flow and diffusion processes in fractured media, the time-step control of the diffusion-dominated matrix processes is often several orders of magnitude greater than that necessary for the stable solution of the advective dominated transport in the fracture. Solving this problem requires a very fine discretization near the fracture–matrix interface [9, 17]. Such mesh refinement significantly increases computational requirements, and may require consideration of grid adaptation algorithms; for example, see Kaiser et al. [18] and Haefner and Boy [19].

An alternative approach avoiding the need for a discrete fracture modeling is the equivalent porous medium concept. The flow in fractures is considered to occur within a clearly defined continuum in contact with a second continuum representing the matrix. Various exchange terms are required to describe the interaction of the continua with each other. Based on this concept, Pruess and Narasimhan [20] presented the double porosity concept, encapsulated in the modeling method MINC, "Multiple INteracting Continua". Pruess [21] states that "MINC can only be applied to media in which the fractures are sufficiently well connected so that a continuum treatment of flow in the fracture network can be made". Several further developments on this approach have been documented, particularly Zimmerman et al. [22] presented a method of linking the matrix storage with the flow in the fractures via a source term in the flow equation which allows the

description of transient exchange processes. Dual continua approaches have also been successfully applied in Karst and contaminant hydrology (e.g., Teutsch [23], Birkholzer [24]).

In many circumstances, definition of equivalent parameters to describe the exchange between the matrix blocks and the fractures provides a powerful tool for the evaluation of large-scale problems such as geothermal fields. However, in a number of cases, applying equivalent exchange parameters to model and predict flow and transport may be missing vital processes such as the effect of channeling. Therefore, the ability to discretely represent the fracture planes allows the effects of different fracture surface profiles to be investigated on the transport signal and key processes to be identified and characterized more accurately.

In this paper, we present a hybrid numerical and analytical model which uses the advantages of both numerical and analytical techniques to analyze flow, transport, and the effects of heterogeneity (roughness) as well as matrix diffusion in a real fracture. The advective dominated transport in the fracture is solved numerically allowing the heterogeneous aperture distribution to be represented. The matrix diffusion is solved analytically and communicates with the numerical advection dominated solution through the use of source/sink terms. The discrete representation of the fracture plane allows the effects of different fracture surface profiles to be investigated. In particular, the effects of increased channeling on matrix diffusion are assessed. The analytical solution for matrix diffusion allows species-dependent chemical and physical parameters to be accounted for and also includes linear sorption. This hybrid numerical and analytical approach, requiring only the fracture to be discretely defined geometrically, allows problems to be solved with significantly less computational cost than standard approaches where both the matrix and the fracture require geometrical definition.

For simplified fracture geometries, the approach has been verified against the analytical matrix diffusion code PICNIC [25] and compared to a numerical solution for two intersecting fractures in a 20 cm block. The method is then demonstrated on two fracture planes representing experimental field conditions in the Grimsel rock laboratory (Switzerland).

2 Modeling approach

The model described here has been integrated into the scientific GeoSys/Rockflow code [26, 27], a standard Galerkin finite element solver [28]. In the fracture, steady state fluid flow is represented by Eq. 1 for a unit volume (e.g., Freeze and Cherry [29])

$$\nabla^T (K \nabla h) = q \tag{1}$$

where K denotes the hydraulic conductivity tensor [$\mathrm{m \cdot s^{-1}}$], h is the hydraulic head [m], and q is source/sink vector [$\mathrm{s^{-1}}$]. This equation is valid for a saturated, non-deforming porous medium with heterogeneous hydraulic conductivity. The solution of Eq. 1 using the finite element technique is covered in standard works such as Istok [30] and Lewis and Schrefler [31].

Because fluid flow in the fracture is approximated as classical Darcy flow, hydraulic conductivity is calculated using the well-known cubic law [32]. This law states that for laminar flow between smooth parallel plates separated by an aperture e [m], the hydraulic conductivity is given by

$$K_i = \frac{e_i^2 \rho g}{12 \mu} \tag{2}$$

where ρ is the fluid density [$\mathrm{kg \cdot m^{-3}}$], g represents gravitational acceleration [$\mathrm{m \cdot s^{-2}}$], and μ is the dynamic viscosity of the fluid [$\mathrm{kg \cdot m^{-1} \cdot s^{-1}}$]. Here, the hydraulic conductivity K_i and the aperture e_i are indexed to indicate that we are using the local cubic law, applying the cubic law at the level of individual fracture elements i. This expression typically overestimates the hydraulic conductivity of rough fractures to some degree, but it provides a first order approximation of the correspondent permeability distribution given a particular aperture distribution [33–35]. We assume this as an approximation as the main focus of this work is not the distribution of flow in a rough fracture, but rather the combination of an analytical solution for matrix diffusion with a numerical solution for flow in an unevenly distributed conductivity field. Using statistical data for the fracture aperture distribution and the autocorrelation, multiple synthetic aperture fields have been generated [36]. The fracture plane is discretized into individual elements, and an aperture e_i is mapped to each element (Fig. 1). From this, the corresponding elemental permeability can be calculated.

Solving Eq. 1 provides the hydraulic head at each node in the finite element model which can be used to calculate the elemental flow velocities. The flow velocities are then used to derive the solution of the transport equation

$$\frac{\partial C}{\partial t} = -\nabla^T (D \nabla C) - v \cdot \nabla C + C_s \tag{3}$$

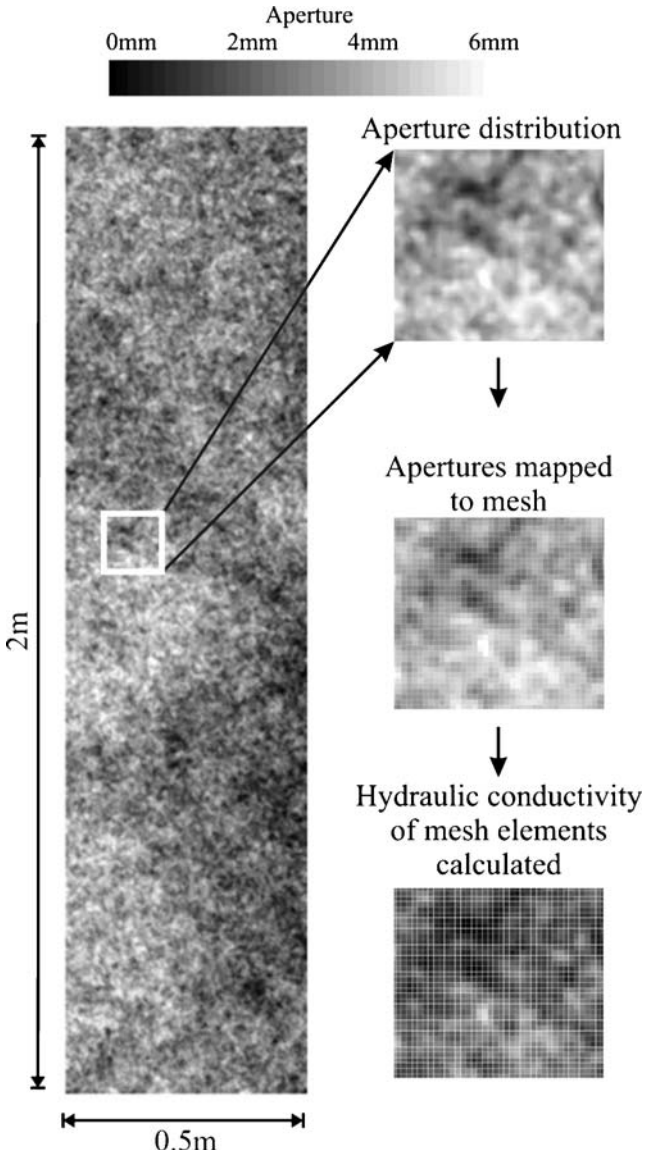

Fig. 1 Geostatistical aperture distribution mapped to fracture plane

where C is the concentration [kg·m^{-3}], D is the dispersion tensor [m^2·s^{-1}], v is the advective velocity [m·s^{-1}], and C_s is a concentration source/sink [kg·m^{-3}·s^{-1}]. This solution is equally applicable to thermal transport in a fracture, for Eq. (3) and all the following key equations concerning equivalent expressions for thermal transport may be found in the Appendix.

The preceding equations describe flow and transport within the fracture. In the surrounding, relatively impermeable rock matrix, different processes dominate the transport of solutes and thermal energy. In the matrix, the transport is largely diffusive rather than advective. If advection can be neglected, matrix transport can be described analytically and linked to the transport in the fracture through source/sink terms. If we assume that the diffusive flux from a fracture is normal to the direction of advective flow, the diffusion profile can be represented by the second order unsteady state diffusion equation, i.e., Fick's second law (4) [37]. Here, the coordinate direction z is the normal to the fracture plane as shown in Fig. 2. The standard solution to this equation for a concentration at a time t and distance z from the source is Eq. 5 [37]. The matrix is assumed to extend to infinity in the region $z > 0$.

$$\frac{\partial C}{\partial t} = D^* \frac{\partial^2 C}{\partial z^2} \tag{4}$$

$$C(z,t) = C_0 erfc\left[\frac{z}{\sqrt{4D^* t}}\right] \tag{5}$$

In Eq. 4, D^* represents the apparent diffusion coefficient [m^2·s^{-1}] [38]. In Eq. 5, C_0 is the boundary concentration at $z = 0$ or, for the purposes of this model, the solute concentration in the adjacent fracture.

Equation (6) represents the superimposition of two equal but oppositely signed inputs offset in time.

$$C(z,t) = C_0 erfc\left[\frac{z}{\sqrt{4D^*(t-t_0)}}\right] - C_0 erfc\left[\frac{z}{\sqrt{4D^*(t-t_1)}}\right] \tag{6}$$

This expression gives the concentration profile at time t, for a pulse of boundary concentration C_0 at coordinate $z = 0$, starting at time t_0 and ending at a time t_1 where $t > t_1 > t_0$ [39]. Generalizing Eq. 6 for $n = 1, 2, 3, \ldots$ pulses gives

$$C(z,t_n) = C_n erfc\left[\frac{z}{\sqrt{4D^*(t_n - t_{n-1})}}\right] + \sum_{j=1}^{n-1}\left\{C_j\left[erfc\left[\frac{z}{\sqrt{4D^*(t_n - t_{j-1})}}\right] - erfc\left[\frac{z}{\sqrt{4D^*(t_n - t_j)}}\right]\right]\right\} \tag{7}$$

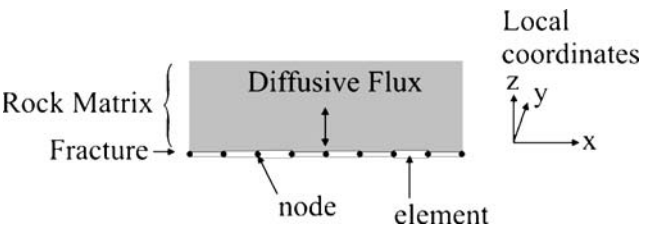

Fig. 2 Local coordinate system for matrix diffusion

where C_n is the boundary (fracture) concentration in time step n (i.e., between times t_{n-1} and t_n), and C_j is the boundary (fracture) concentration between times t_{j-1} and t_j. This formulation also assumes steady state conditions within each time step.

The term source/sink term C_s in Eq. 3 provides the link between the two-dimensional advective–dispersive transport in the fracture and the one-dimensional diffusive transport in the matrix. This term represents the rate of solute mass transfer between the fracture and the matrix divided by the volume of a given local fracture element (or nodal patch). Using Fick's first law of diffusion [37] for steady state conditions, it provides the following expression for C_s

$$C_{\mathrm{s}} = -\frac{D^* A_i}{V_i}\frac{\partial C}{\partial z} = -\frac{D^*}{e_i}\frac{\partial C}{\partial z} \tag{8}$$

where A_i is the area of the fracture wall occupied by element i and V_i is the volume of element i. This is assuming the concentration gradient remains the same for the discretized time step chosen in the model simulations. This expression represents the source term contribution matrix via the fracture wall to the fracture. Where the contribution of two fracture walls to the fracture element is required, this expression can be multiplied by 2. The term $\partial C/\partial z$ represents the gradient of the concentration in the matrix forming the fracture wall. Flux into and out of the fracture is controlled by this gradient. This term is found by partially differentiating Eq. 7 with respect to z. As we are only interested in the concentration gradient at the interface, the formulation for $\partial C/\partial z$ can be simplified by setting the coordinate z equal to zero, providing the following expression

$$\begin{aligned}\frac{\partial C\,(z=0,t_n)}{\partial z} = {} & \frac{-C_n}{\sqrt{\pi D^*\,(t_n - t_{n-1})}} \\ & + \sum_{j=1}^{n-1}\left\{\frac{-C_j}{\sqrt{\pi D^*\left(t_n - t_{j-1}\right)}}\right. \\ & \left. + \frac{C_j}{\sqrt{\pi D^*\left(t_n - t_j\right)}}\right\}\end{aligned} \tag{9}$$

Depending on the terms included in the calculation of the diffusive term D^*, it is possible to examine both the effects of matrix diffusion alone and matrix diffusion combined with sorption processes. Following Grathwohl [38], diffusion in the matrix is defined according to

$$D^* = \frac{D_{\mathrm{aq}}}{R\tau} \tag{10}$$

where D_{aq} is the aqueous diffusion coefficient [$\mathrm{m^2 \cdot s^{-1}}$], R is the retardation factor [–], and τ is the tortuosity factor of the porous rock matrix [–]. The tortuosity factor cannot be measured independently, but is often estimated from the porosity ε, i.e., $\tau = \varepsilon^{1-m}$, where $m \approx 2$ [40]. If one wishes to consider matrix diffusion alone, then R is set equal to one. To assess the effects of sorption, the variable R can be expressed as

$$R = 1 + \frac{K_{\mathrm{d}}\rho}{\varepsilon} \tag{11}$$

where K_d is the solute distribution coefficient [$\mathrm{m^3 \cdot kg^{-1}}$] (i.e., the ratio of sorpted to dissolved concentrations) and ρ is the bulk density of the rock matrix [$\mathrm{kg\ m^{-3}}$]. Equations (10) and (11) assume a linear sorption isotherm, instantaneous equilibrium sorption, and that the proportion of dead end or blind pores is negligible. For non-linear sorption calculations, K_d is not constant, and the depth-dependent concentration of the chemical species in the fracture wall is required. It is possible to calculate this concentration profile from Eq. 7, but the solution of non-linear sorption would require additional computational resources, and is beyond the scope of this work. A more detailed consideration of sorption phenomena can be found in Grathwohl [38].

In addition to the Courant and Neumann stability criteria discussed in Section 1, one further stability criterion must be satisfied for the stability of the numerical component of this hybrid model. Known as the "well criterion", this condition expresses the fact that within one time step a source term may not take more mass, or energy, from a nodal patch or element than is present at the start of the time step [41]. For the source terms C_s, the well stability criterion is

$$\frac{\Delta mass}{mass} = \frac{C_{\mathrm{s}} V_i \Delta t}{C_i V_i} = \frac{-2D^*\partial C_i/\partial z}{e_i C_i}\Delta t \le 1 \tag{12}$$

It is possible to violate this criterion if either D^* is very large, e_i is very small, or the time-step length Δt is large. For the purposes of this work, the problem of small e_i values is most significant. When the measured statistics of the fracture aperture distribution are represented explicitly, it is inevitable that some of the elements comprising the fracture must have small apertures. The smaller the aperture of the fracture, the smaller is the amount of mass actually present in the corresponding fracture element, and therefore the smaller is the amount of mass which can be removed in any given time step.

The problem arises because the concentration gradient at the fracture–matrix interface, $\partial C / \partial z$ is calculated from the previous time step and it is used to predict the fracture–matrix diffusive exchange in the

current time step. In reality, this gradient, $\partial C / \partial z$, will go to zero before the concentration in the fracture becomes zero or negative. In this model, we apply a time discretization and assume constant gradient within each time step. This is a reasonable assumption for most cases where the concentration reached at the start of the next time step is not known. However, in the case where all the mass in an element could be removed, we know that the lower limit of concentration is going to be the value of concentration in the fracture that ensures the gradient $\partial C / \partial z$ in the fracture wall is zero at the end of the time step. Expressing this in other terms: As the mass is diffusing into the matrix, the concentration in the fracture will drop until the concentration in the fracture and the matrix is equal and no further.

Using Eq. 7, it is possible to define the concentration in the fracture at which there will be no more flux into or out of the matrix for the current time step (C_g). Defining H as

$$H = \sum_{j=1}^{n-1} \left\{ \frac{-C_j}{\sqrt{\pi D^* \left(t_n - t_{j-1}\right)}} + \frac{C_j}{\sqrt{\pi D^* \left(t_n - t_j\right)}} \right\} \quad (13)$$

allows us to express this concentration as

$$C_g = H\sqrt{\pi D^* \left(t_n - t_{n-1}\right)} \quad (14)$$

therefore, the maximum change in concentration which could occur, ΔC, is from the current concentration C_t to C_g. Given the boundary condition of the system for this time step and element is known, i.e., the concentration in the matrix, we can apply a 1D analytical solution to determine how much mass actually will enter the element in the given time step. This solution allows for the fact that the gradient will be changing significantly in the given time step. Applying the 1D analytical solution, we see that for a Dirac pulse at $z = 0$

$$C\left(t\right) = \frac{M}{2\sqrt{\pi Dt}} \quad (15)$$

Setting $t = 1$ and the normalized concentration at $C(t = 1) = 1$, then the concentration at time $t + \Delta t$ is given by

$$C_{(\Delta t)} = \frac{1}{\sqrt{1 + \Delta t}} \Delta C \quad (16)$$

Using this approach, the mass to be removed from the cells can be calculated as $C_t - C_{t+\Delta t}$ multiplied by the volume represented by the node.

Examining Eq. 9, one can see that, to complete the summation, past concentration information is required for every preceding time step at every node. For large fracture networks with many elements, and long-term tests with many thousands of time steps, the data requirements can become substantial. To mitigate this problem, two facts can be considered. First, as the time difference between the current time and the initiation time of a preceding matrix diffusion pulse increases, the influence of the older pulse becomes less significant. If one assumes a constant time step length, an expression for the relative absolute contribution of a pulse to the concentration gradient at the interface can be derived from Eq. 9 to yield

$$relative\_contribution = \left(\frac{1}{\sqrt{k}} - \frac{1}{\sqrt{k+1}} \right) \quad k = 1, 2, \ldots \quad (17)$$

where k is the number of time steps since the end of the pulse. From this, we see that after ten time steps, the contribution of a pulse to the gradient is only 1.5% of its initial value, after 100 time steps the relative contribution is less than 0.05%, and after 1,000 time steps the relative contribution is less than 0.002%. Thus, it is possible to cap the required computational resources while maintaining a sufficient level of accuracy. The second option to control the computational requirements is to reduce the resolution of the pulse history. The frequency at which C_s is recalculated must not necessarily be the same as the time-step frequency. It was found that the pulse history could be averaged over several time steps without affecting the integrity of the results, as long as the characteristics of the pulse were captured. In terms of implementation, we introduced a resolution, indicating that the concentration source term should only be recalculated at every nth time step. The required sampling resolution depends largely on the rate at which the concentration in the fracture element is changing and on other factors such as the length of tracer injection pulses.

3 Verification

In order to verify the computational model, numerical simulations using the hybrid analytical–numerical scheme implemented in GeoSys/Rockflow were compared to predictions produced by the transport code PICNIC (PSI/QuantiSci Interactive Code for Networks of Interconnected Channels) [25]. The latter code has been developed within the framework of the Swiss Radionuclide Retardation Programme for the assessment of radionuclide migration. The underlying conceptual model for PICNIC envisions flow in a fractured rock mass as occurring within a network of legs which interact only at the junctions. Within the legs, which

Table 1 Geometry and material properties used for the verification calculations in both the hybrid model (GeoSys/Rockflow) and the analytical model (PICNIC)

Symbol	Description	Value	Hybrid scheme	PICNIC
L [m]	Distance between injection boundary and observation transect	2.5	X	X
α_T [m]	Transverse dispersion	0.1	X	
ρ [kg m^{-3}]	Bulk matrix density	2,670	X	X
e [m]	Fracture aperture	0.55×10^{-3}	X	X
v[m s^{-1}]	Fluid velocity	7.05×10^{-4}	X	X
α_L [m]	Longitudinal dispersion	0.1	X	
Pe [–]	Peclet number (PICNIC only)	25		X
ε [–]	Matrix porosity	0.3	X	X
D^* [m^2 s^{-1}]	Diffusion constant in rock matrix	7.4×10^{-11}	X	X

represent individual fractures, flow and matrix diffusion equations are solved analytically using Laplace transformation as described by [14] and [12]. In the PICNIC model, advective–dispersive transport in the fracture is calculated based on a constant fluid velocity within the fracture and a dispersion length corresponding to a Peclet number of 25. As previously stated, fluid flow in the porous matrix is disregarded and only the diffusion into the pore space and retardation caused by a linear sorption isotherm are considered. In the experiment, a tracer was injected into the fracture system at a constant rate for the first 50 s. The breakthrough of the tracer was observed at a distance of 2.5 m downstream. The experimental system was set up such that the downstream transport boundary was sufficiently distant that it did not influence the tracer breakthrough. This was done because, unlike the hybrid model, the analytical solution used by PICNIC assumes that the fracture has an infinite downstream extent. The input parameters used in both the GeoSys/Rockflow and PICNIC simulations correspond to the parameters published by Kosakowski and Smith [42] and are presented in Table 1. Figure 3 illustrates the breakthrough curves calculated by the two codes for advective–dispersive transport in the fracture (AD), for advective–dispersive transport with matrix diffusion (AD MD), and for advective–dispersive transport with matrix diffusion and linear sorption in the matrix (AD MD Sp). The agreement between the two models is very good.

4 Comparison to a numerical model

To enable a comparison of the implementation of the hybrid method to purely numerical methods, solute transport through a discretely fractured block of dimensions 20 × 20 cm was simulated. The block contains two fractures which join in the middle. Here, the fracture is represented by discrete elements whose thickness is related to the fracture permeability. These may be obtained from experimental data or may be generated using a statistical approach (e.g., Walsh et al. [43]). Figure 4 illustrates the model setup and the geometrical comparison between the purely numerical and the hybrid approach. The numerical models consists of 161,309 triangle elements in order to discretize the fracture intersection; the hybrid analytical–numerical model requires 5,709 triangle elements. The analytical–model presented in this paper is a 1D model assuming infinite extent of the matrix continuum, and therefore

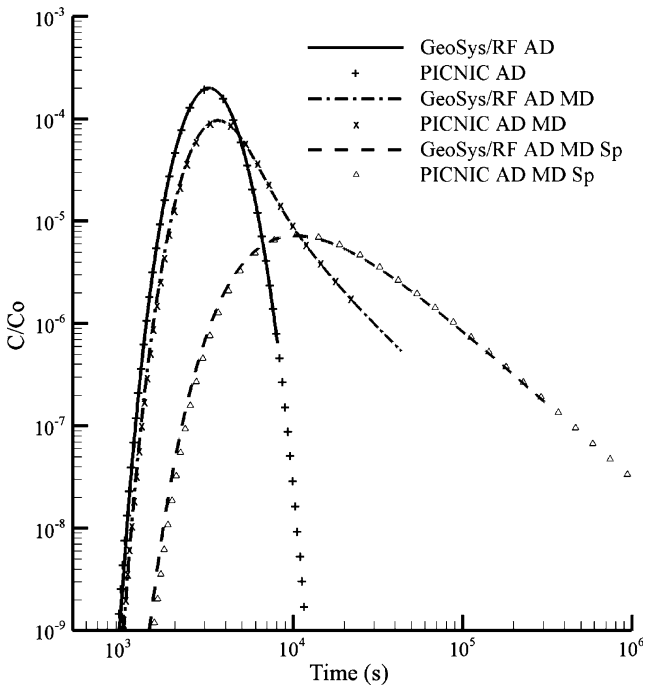

Fig. 3 Comparison of breakthrough curves for the verification test case calculated using the hybrid model (GeoSys/Rockflow) and analytical model (PICNIC). Results are (1) for advective–dispersive transport only (*AD*), (2) for AD and matrix diffusion (*MD*), and (3) for AD with MD and linear sorption (*Sp*)

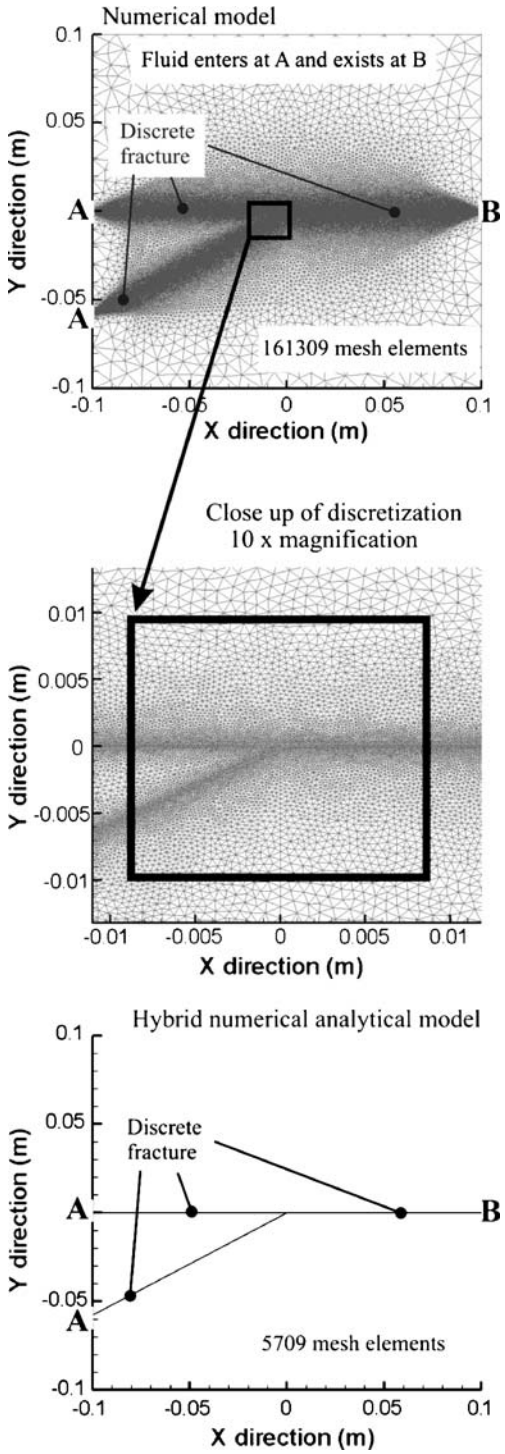

Fig. 4 Comparison of a numerical and hybrid analytical and numerical approach to modeling fluid flow in two intersecting fractures in a block 20 × 20 cm

in the vicinity of the fracture intersection this condition breaks down. In further work, the development and implementation of hybrid models to cover such circumstances will be discussed. However, this model geometry is deliberately chosen to demonstrate the flexibility of the approach, examine differences in the modelling results, and to illustrate that the combination of the analytical and numerical methods provides an excellent alternative as a tool for understanding the behavior of the fracture systems. Figure 5 gives the comparison of the results, and it can be seen that the curves are almost identical. The computational expense of the hybrid approach, however, is almost a factor of 10 less in comparison to the purely numerical method for this case.

5 Demonstration example

Having verified that the hybrid method is able to reproduce the results of the analytical solution to a sufficient degree of accuracy, the hybrid model is now applied to heterogeneous fractures. This type of problem cannot be handled using analytical solutions; however, a pure numerical solution for both the advective dominated transport in the fractures and the matrix diffusion in the rock is complicated due to the extremely different length scale of both processes. A numerical solution would require extremely fine meshes for accuracy. Therefore, the hybrid approach is an appropriate solution method for this type of multi-scale problem [44].

Mettier et al. [36] presents the results of aperture measurements from a 5.2-m section of the shear zone at the Grimsel site. The geostatistical parameters of the fractures surfaces are reported as being a minimum of aperture of 1×10^{-5} m and a maximum aperture of 0.02 m, representing a permeability distribution of 8×10^{12} m^2 to 3×10^{-5} m^2, and a standard deviation of 0.8 for the $\log_{10}$ of the apertures with an average aperture size of 4×10^{-4} m. Using a fracture generator

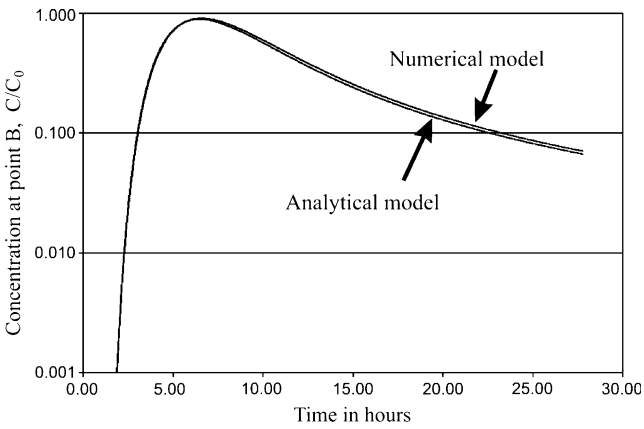

Fig. 5 Comparison of the results of a numerical and hybrid analytical and numerical approach to modeling solute transport in two intersecting fractures in a block 20 × 20 cm

discussed in Walsh et al. [43] based on a fractal representation of the fracture plane, we generated two artificial fracture surfaces with apertures ranging from 1×10^{-5} m to 0.008 m, representing a permeability range of 8×10^{-12} m^2 to 6×10^{-6} m^2. We achieved a standard deviation for the $\log_{10}$ of the apertures of 0.36 with an average aperture of 3 mm. A larger variance as suggested by Mettier et al. [36] could only be achieved with the fractal generator by increasing the average aperture width significantly beyond the field values. The two fractures with slightly different statistical properties are presented in Table 2.

The artificial fracture surfaces measured 0.5×2.00 m at a resolution of circa 4 mm resulting in a 65,000-element grid. The hydraulic boundary conditions were set to mimic a realistic flow situation along the 2 m length of the fracture under field conditions. The upper boundary, deemed the "outflow edge" of the fracture, was set as constant zero hydraulic head, and the "inflow edge" of the fracture was given a minimal head of 0.1 mm, i.e., seepage conditions were represented. These simple boundary conditions ensure a steady state hydraulic flux from the bottom of the fracture to the top. Tracer is injected as a 180 s pulse of constant concentration at the base of the fracture. The hydraulic outflow edge was left to default as a zero gradient mass transport boundary. The breakthrough curves were recorded as a flux-weighted response across the outflow edge of the fracture, as would be measured in seepage across the outcropping width of the fracture under field conditions.

In order to compare the influence of the heterogeneity and the effect of matrix diffusion [1], we performed the exact same realizations twice, once with and once without the analytical solution for matrix diffusion for both fracture planes. Such methodology could be expanded to investigate the use of a single effective matrix diffusion coefficient to predict breakthrough curves in a fractured formation as discussed by Zhang et al. [5] but is beyond the scope of this work.

Table 2 Fracture plane statistics used for demonstration of methodology

	High variance	Low variance
Fracture surface statistics		
Fractal dimension [–]	2.5	2.5
Standard deviation surface roughness [mm]	15.0	15.0
Mismatch wavelength [mm]	10.0	10.0
Maximum degree of correlation between top and bottom surfaces [–]	0.97	0.98
Aperture statistics		
Average [mm]	3.08	2.90
Standard deviation [mm]	1.34	1.24
Contact ratio [–]	0.012	0.011
Permeability statistics		
Average [m^2]	9.41E-07	8.28E-07
Standard deviation [m^2]	7.25E-07	6.33E-07
Variance of $\log_{10}$ [permeability] [–]	0.52	0.49

6 Results and discussion

The breakthrough curves for the two fracture plane realizations with and without matrix diffusion are illustrated in Fig. 6 for two cases; a lower (LV) and a higher variance (HV) of fracture surface statistics. In Fig. 7, the time-dependent distribution of the pulse for the higher variance fracture can be seen with and without matrix diffusion. Here, we note that the modeling conditions are identical apart from the aperture distributions on the fracture planes. Based on this demonstration example, we note a number of significant features discussed below.

Comparing first the non-matrix diffusion (MD) curves of the simulations (Fig. 6), flow in the slightly higher variance fracture (HV) results in more pronounced channeling and the development of preferential flow paths. The flow in the slightly lower variance fracture (LV) demonstrates a smoother, more homogeneous breakthrough curve. The higher variance

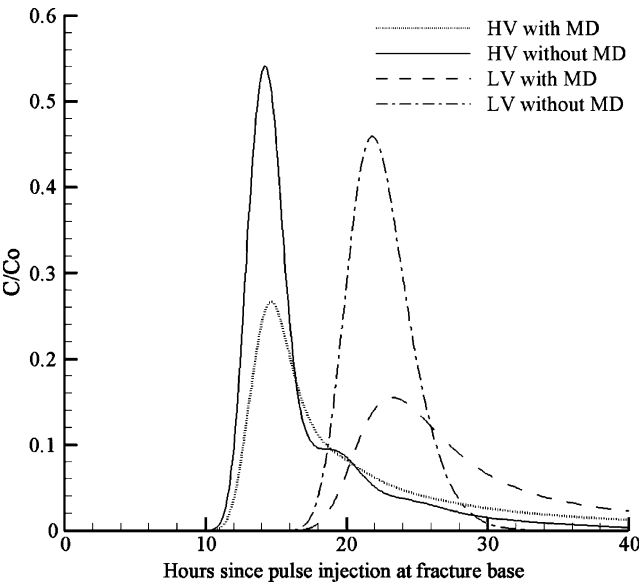

Fig. 6 Breakthrough curves for a heterogeneous fracture realization. *HV* Higher variance, *LV* lower variance, *MD* matrix diffusion

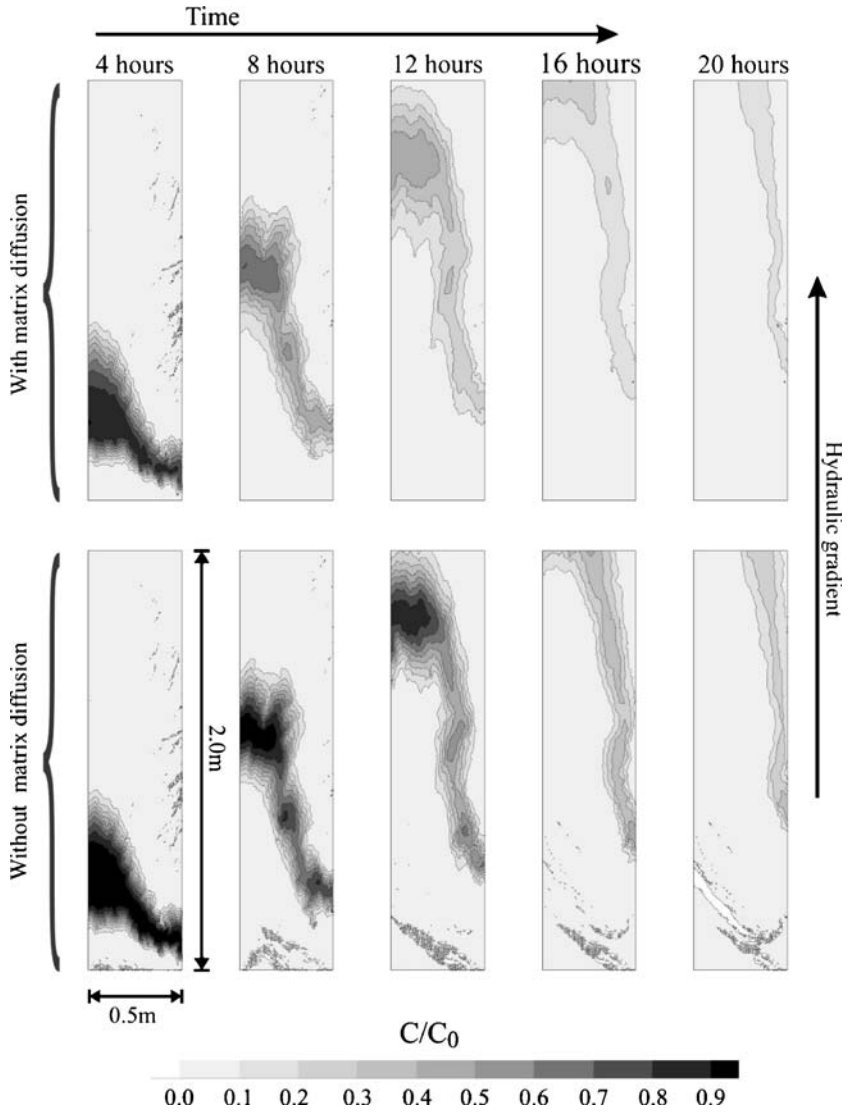

Fig. 7 Time series of a tracer cloud moving through the higher variance realization of the fracture, with (*top*) and without (*bottom*) matrix diffusion

curve demonstrates a double peak arrival due to flow channeling. The first peak arrival of the higher variance curve is 150% earlier than that of the peak in the lower variance curve, although the arithmetic average hydraulic conductivity is only 15% more than the lower variance fracture. This trend would be as expected when considering the effects of increasing roughness and the development of channeling. What is also of interest is the long tailing developed in the higher variance fracture in comparison to the lower variance fracture. This is due to slow movement of tracer in low conductivity channels of the fracture. In reality, such an effect could be mistaken as matrix diffusion.

Examining now the matrix diffusion-influenced curves, matrix diffusion both retards the arrival of the tracer at the outflow boundary and smoothes the curves. In the higher variance case, the retardation is less for the more rapid flow in the preferential flow channels in comparison to lower variance fracture; through smoothing of the curve, the double peak, i.e., the clear demonstration of preferential flow paths, is lost. Comparing the higher variance and lower variance fractures with matrix diffusion, the difference between the signals becomes little more than a difference in the long-term tailing, although the flow and transport processes are significantly different due to the channelling.

Should such curves have been retrieved from the field, fitting by application of general dispersion/diffusion parameter and equivalent matrix diffusion parameters would not necessary indicate that the details of the flow and transport processes have been properly determined. Should sorption also be included, then a further intermixing of the processes and their individual signals will occur. Exactly these matrix diffusion processes and sorption processes need to be accurately

characterized when matrix diffusion forms an important part of engineered design.

7 Conclusions

A new hybrid analytical and numerical modeling technique is presented which combines the advantages of analytical and numerical approaches to model mass transport in heterogeneous fractures. The numerical model solves flow and mass transport in the fracture and the analytical model represents the continuum-based matrix diffusion process. Through the use of source/sink terms, the diffusive flux in and out of the matrix is included. Using this approach, there is no need to conform strictly to the Neumann stability criteria in the matrix and there is also no necessity of the three-dimensional mesh representation of the matrix with the accompanying intensive computational demands. The stability criteria controlling the size of the source terms, the "well criteria", is adhered to by constantly monitoring the size of this term and applying either a steady state solution where the end boundary conditions are not known or a non-steady state solution where the boundary conditions are known, i.e., the concentration/energy in the fracture equals the concentration/energy in the fracture wall. Only the advective flow in the fractured rock defines the limits of the numerical solution. This allows the discrete features of the fractures to be represented numerically as a two-dimensional aperture and permeability distribution.

The analytical solution for matrix diffusion is developed for mass transport of contaminants, and can be applied to both conservative and linearly sorbing species. The application of the same solution to heat transport is given in the Appendix. The solution procedure has been verified against an analytical solution for simple fracture–matrix geometry, and compared to a numerical solution for two intersecting fractures in a 20 cm block.

To demonstrate the use of the modeling approach, two fracture planes, 2×0.5 m, were generated based on experimental data from a Grimsel shear zone. The effect of the variance (related to roughness) and the effect of matrix diffusion on the flow and mass transport in these fractures were demonstrated by simulating the movement of a tracer pulse through the fractures due to seepage. The predicted tracer breakthrough curves were such that had they been retrieved from the field and fitted by application of general dispersion/diffusion and equivalent matrix diffusion parameters, the details of the flow and transport processes would not have been properly determined. Had sorption been included in the simulation, the individual process signals would have been further mixed. However, exactly these matrix diffusion and sorption processes need to be accurately characterized when they form an important part of engineered design.

This modeling approach reduces the computational power needed to investigate the long-term effects of matrix diffusion. Additionally, the discrete analysis of the fracture surfaces allows species and porosity variations to be modeled individually rather than requiring the introduction of general effective parameters.

Currently, the matrix diffusion term assumes an unlimited depth of penetration in the matrix blocks. However, further development of the analytical solution will allow different scenarios to be addressed.

The hybrid analytical–numerical technique presented here is a useful tool for the investigation of complicated fracture systems and the interaction of several coupled processes.

Acknowledgements The authors gratefully acknowledge the German Science Foundation (Deutsche Forschungsgemeinschaft) for funding of this work (MC 113/1-5).

Appendix: Thermal equations

Nomenclature

c	Heat capacity (J/kg K)
ρ	Density (kg/m^3)
λ	Thermal conductivity (J/K m s)
D^*	Energy diffusion dispersion tensor (m^2/s)
T_s	Heat source (J/m^3 s)
t	Time (s)
T	Temperature (K)
v	Velocity (m/s)
z	m in z direction

Superscripts

m	Equivalent value for porous medium
w	Water

Energy balance equation $c\rho\frac{dT}{dt} = \lambda^m \nabla^2 T - c^w \rho^w v \cdot \nabla T - T_s$

Diffusion of a temperature pulse $T(z,t) = T_0 erfc\left[\frac{z}{\sqrt{4D^*(t-t_0)}}\right] - T_0 erfc\left[\frac{z}{\sqrt{4D^*(t-t_1)}}\right]$

Definition of thermal diffusion coefficient $D^* = \frac{\lambda^m}{\rho^m c^m}$

Analytical matrix diffusion term

$$T(z,t_n) = T_n erfc\left[\frac{z}{\sqrt{4D^*(t_n - t_{n-1})}}\right] + \sum_{j=1}^{n-1}\left\{T_j\left[erfc\left[\frac{z}{\sqrt{4D^*(t_n - t_{j-1})}}\right] - erfc\left[\frac{z}{\sqrt{4D^*(t_n - t_j)}}\right]\right]\right\}$$

Calculation of source term $T_s = -\frac{2D^* A_i}{V_i}\frac{\partial T}{\partial z} = -\frac{2D^*}{e_i}\frac{\partial T}{\partial z}\rho^m c^m$

Transient analytical solution for stability criteria

$$T_{(\Delta t)} = \frac{1}{\sqrt{1+\Delta t}}\Delta T$$

References

1. Jacob, A.: Matrix diffusion for performance assessment—experimental evidence, modeling assumptions and open issues. Paul Scherrer Institute (2004)
2. Min, K., Rutqvist, J., Tsang, C.F., Jing, L.: Stress-dependent permeability of fractured rock masses: a numerical study. Int. J. Rock Mech. Min. Sci. **41**, 1191–1210 (2004). doi:10.1016/j.ijrmms.2004.05.005
3. Taylor, L.W., Polard, D.D., Aydin, A.: Fluid flow in discrete joint sets: field observations and numerical simulations. J. Geophys. Res. **104**(B12), 28983–29006 (1999). doi:10.1029/1999JB900179
4. Chen, C.Y., Horne, R.N., Fourar, M.: Experimental study of liquid–gas flow structure effects on relative permeabilities in a fracture. Water Resour. Res. **40**(8), W083011–W0830115 (2004). doi:10.1029/2004WR003026
5. Zhang, Y., Liu, H., Zhou, Q., Finsterle, S.: Effects of diffusive property heterogeneity on effective matrix diffusion coefficient for fractured rock. Water Resour. Res. **42**, 1–8 (2006)
6. Park, C.-H., Beyer, C., Bauer, S., Kolditz, O.: A study of preferential flow in heterogeneous media using random walk particle tracking. Geosciences J. **12**(3), 285–297 (2008). doi:10.1007/s12303-008-0029-2
7. Berkowitz, B.: Characterizing flow and transport in fractured geological media: a review. Adv. Water Resour. **25**, 861–884 (2002). doi:10.1016/S0309-1708(02)00042-8
8. Sanchez-Vila, X., Carrera, J.: On the striking similarity between the moments of breakthrough curves for a heterogeneous medium and a homogeneous medium with a matrix diffusion term. J. Hydrol. (Amst.) **294**, 164–175 (2004). doi:10.1016/j.jhydrol.2003.12.046
9. Carrera, J., Sánchez-Vila, X., Benet, I., Medina, A., Galarza, G., Guimerà, J.: On matrix diffusion: formulations, solution methods and qualitative effects. Hydrogeol. J. **6**, 178–190 (1998). doi:10.1007/s100400050143
10. Kosakowski, G.: Anomalous transport of colloids and solutes in a shear zone. J. Contam. Hydrol. **72**, 23–46 (2004). doi:10.1016/j.jconhyd.2003.10.005
11. Grisak, G.E., Pickens, J.F.: An analytical solution for solute transport through fractured media with matrix diffusion. J. Hydrol. (Amst.) **52**, 47–57 (1981). doi:10.1016/0022-1694(81)90095-0
12. Tang, D.H., Frind, E.O., Sudicky, E.A.: Contaminant transport in fractured porous media; analytical solution for a single fracture. Water Resour. Res. **17**(3), 555–564 (1981). doi:10.1029/WR017i003p00555
13. Sudicky, E.A., Frind, E.O.: Contaminant transport in fractured porous media—analytical solutions for a system of parallel fractures. Water Resour. Res. **18**(6), 1634–1642 (1982). doi:10.1029/WR018i006p01634
14. Barker, J.A.: Laplace transform solutions for solute transport in fissured aquifers. Adv. Water Resour. **5**(2), 98–104 (1982). doi:10.1016/0309-1708(82)90051-3
15. Tidwell, V.C., Meigs, L.C., Christian-Frear, T., Boney, C.M.: Effects of spatially heterogeneous porosity on matrix diffusion as investigated by X-ray absorption imaging. J. Contam. Hydrol. **42**, 285–302 (2000). doi:10.1016/S0169-7722(99)00087-X
16. Neuman, S.P.: Trends, prospects and challenges in quantifying flow and transport through fractured rocks. Hydrogeol. J. **13**(1), 124–147 (2004). doi:10.1007/s10040-004-0397-2
17. Kolditz, O., Clauser, C.: Numerical simulation of flow and heat transfer in fractured crystalline rocks: application to the hot dry rock site in Rosemanowes (U.K.). Geothermics **27**(1), 1–23 (1998). doi:10.1016/S0375-6505(97)00021-7
18. Kaiser, R., Rother, T., Kolditz, O., Zielke, W.: Automatic grid adaptation for modeling coupled flow and transport processes in fractured aquifers, Computational methods in water resources—Volume 1—Computational methods for subsurface flow and transport, 279–283 (2000)
19. Haefner, F., Boy, S.: Fast transport simulation with an adaptive grid refinement. Ground Water **41**(2), 273–279 (2003). doi:10.1111/j.1745-6584.2003.tb02590.x
20. Pruess, K., Narasimhan, T.N.: A practical method for modeling fluid and heat flow in fractured porous media. Soc. Pet. Eng. J. **25**(1), 14–26 (1985), February
21. Pruess, K.: Brief guide to the MINC-method for modeling flow and transport in fractured Media, Report LBL-32195, Earth Sciences Division, Lawrence Berkeley Laboratory, University of California, Berkeley, California 94720 (1992)
22. Zimmerman, R.W., Chen, G., Bodvarsson, G.S.: A dual-porosity reservoir model with an improved coupling term, Proceedings Seventeenth Workshop on Geothermal Reservoir Engineering Stanford University, Stanford, California, January 29–31 (1992)
23. Teutsch, G.: Grundwassermodelle im Karst: Praktische Ansätze am Beispiel zweier Einzugsgebiete in tiefen und seichten Malmkarst der Schwäbischen Alb, PhD thesis, Universität Tübingen (1988)
24. Birkholzer, J.: Numerische Untersuchungen zur Mehrkontinuumsmodellierung von Stofftransportvorgängen in Kluftgrundwasserleitern. PhD thesis, Mitteilungen des Instituts für Wasserbau und Wasserwirtschaft, Band 93, RWTH Aachen (1994)
25. Barten, W., Robinson, P.C.: Contaminant transport in fracture networks with heterogeneous rock matrices: The PICNIC code, PSI Report Nr. 01–02, February 2001, ISSN 1019-0643 (2001)
26. Kolditz, O., Bauer, S.: A process-orientated approach to compute multi-field problems in porous media. Int. J. Hydroinformatics **6**, 225–244 (2004)
27. Kalbacher, T., Mettier, R., McDermott, C., Wang, W., Kosakowski, G., Taniguchi, T., Kolditz, O.: Geometric modelling and object-oriented software concepts applied to a heterogeneous fractured network from the Grimsel rock laboratory. Comput. Geosci. **11**(1), 9–26, (2007), March 2007

28. Huyakorn, P.S., Pinder, G.F.: Computational Methods in Subsurface Flow. Academic, New York (1983)
29. Freeze, R.A., Cherry, J.A.: Groundwater. Prentice Hall, Englewood Cliffs (1979)
30. Istok, J.: Groundwater Modeling by the Finite Element Method. Water Resources Monograph. American Geophysical Union, 2000 Florida Avenue, NW, Washington, DC 20009 (1989)
31. Lewis, R.W., Schrefler, B.A.: The Finite Element Method in the Static and Dynamic Deformation and Consolidation of Porous Media. Wiley, Chichester (1998)
32. Witherspoon, P.A., Wang, J.S.Y., Iwai, K., Gale, J.E.: Validity of cubic law for fluid flow in deformable rock fracture. Water Resour. Res. **16**(6), 1016–1024 (1980). doi:10.1029/WR016i006p01016
33. Dijk, P.E., Berkowitz, B.: Three-dimensional flow measurements in rock fractures. Water Resour. Res. **35**(12), 3955–3959 (1999). doi:10.1029/1999WR900200
34. Konzuk, J.S., Kueper, B.H.: Evaluation of cubic law based models describing single-phase flow through a rough-walled fracture. Water Resour. Res. **40**(2), W02402 (2004). doi:10.1029/2003WR002356
35. Nicholl, M.J., Rajaram, H., Glass, R.J., Detwiler, R.: Saturated flow in a single fracture: evaluation of the Reynolds equation in measured aperture fields. Water Resour. Res. **35**(11), 3361–3374 (1999). doi:10.1029/1999WR900241
36. Mettier, R., Kosakowski, G., Kolditz, O.: Influence of small-scale heterogeneities on contaminant transport in fractured crystalline rock. Ground Water **44**(5), 687–696 (2006)
37. Fetter, C.W.: Contaminant Hydrogeology. Prentice-Hall, Upper Saddle River (1993)
38. Grathwohl, P.: Diffusion in Natural Porous Media: Contaminant Transport, Sorption/Desorption and Dissolution Kinetics. Kluwer, Dordrecht (1998)
39. Häfner, F., Sames, D., Voigt, H.-D.: Wärme- und Stofftransport - Mathematische Methoden. Springer, Berlin (1992)
40. Kleineidam, S., Ruegner, H., Grathwohl, P.: Impact of grain scale heterogeneity on slow sorbtion kinetics. Environ. Toxicol. Chem. **18**(8), 1673–1678 (1999). doi:10.1897/1551-5028(1999)018<1673:IOGSHO>2.3.CO;2
41. Kolditz, O.: Non-linear flow in fractured rock. Int J. Numer. Methods Fluid Heat Transp. **11**(6), 547–576 (2001). doi:10.1108/EUM0000000005668
42. Kosakowski, G., Smith, P.: Modeling the transport of solutes and colloids in the Grimsel Migration shear zone. PSI Report Nr. 05-03, Paul Scherrer Institut, Villigen, Switzerland, and Nagra Technical Report 04-01, Wettingen, Switzerland (2005)
43. Walsh, R., McDermott, C., Kolditz, O.: Numerical modeling of stress–permeability coupling in rough fractures. J. Hydrogeology **16**(4), 613–627 (2008). doi:10.1007/s10040-007-0254-1
44. McDermott, C.I., Tarafder, S.A., Schüth, C.: Vacuum assisted removal of volatile to semi volatile organic contaminants from water using hollow fiber membrane contactors II: A hybrid numerical–analytical modeling approach. J. Membr. Sci. **292**(1–2), 17–28 (2007). doi:10.1016/j.memsci.2007.01.009